Wide-Bandwidth Near-Infrared Avalanche Photodiode Photo-receiver

Michael A. Krainak, Guangning Yang, Xiaoli Sun, Wei Lu
NASA Goddard Space Flight Center

Xiaogang Bai, Ping Yuan, Paul McDonald, Joseph Boisvert,
Robyn Woo, Kam Wan, Rengarajan Sudharsanan
Boeing Spectrolab

Abstract-Ultra-sensitive near-infrared optical receivers are required for active optical instruments. The NRC Earth science decadal lidar-based missions including ICESat2, DESDynI, LIST, ASCENDS, ACE and 3D-WINDS and Satellite Laser Ranging will all greatly benefit from high quantum efficiency, very low-noise (near single photon sensitive) optical receivers. Improvements in detector quantum efficiency translate directly to reduced laser energy requirements for active laser instruments. This minimizes spacecraft resource requirements (mass, power, volume) and greatly enhances laser and system reliability. Boeing-Spectrolab and NASA-GSFC are developing a high performance linear mode InAlAs avalanche photodiodes (APD) operating at 1.06 µm. The APD detector will be integrated with transimpedance amplifiers (TIAs) and assembled into a receiver. The overall bandwidth will be greater than 1 GHz, while the noise-equivalent-power (NEP) is reduced to less than 300 fW/√Hz. To minimize the dark current and noise, an InAlGaAs quaternary absorber is being used for high quantum efficiency at 1 µm. The high bandwidth detectors are compatible with newly developed very short pulse (< 1 nanosecond) high-repetition rate (10 kHz) high efficiency (> 15% wall-plug) lasers.

I. INTRODUCTION

In 2007 the National Research Council (NRC), responded to requests from the National Aeronautics and Space Administration (NASA) Office of Earth Science, the National Oceanic and Atmospheric Administration (NOAA) National Environmental Satellite Data and Information Service (NESDIS), and the U.S. Geological Survey (USGS) Geography Division to conduct a decadal survey to generate consensus recommendations from the Earth and environmental science and applications communities regarding a systems approach to space-based and ancillary observations that encompasses the research programs of NASA; the related operational programs of NOAA; and associated programs such as Landsat, a joint initiative of USGS and NASA. The NRC recommended a total of fifteen missions[i] with benefits range from information for short-term needs, such as weather forecasts and warnings for protection of life and property, to the longer-term scientific understanding necessary for future applications that will benefit society in ways still to be realized. Three out of the fifteen recommended missions are laser based instrument for topography mapping of the Earth's surface. These are the Ice, Cloud, and Land Elevation Satellite-II (ICESat-II), Deformation, Ecosystem Structure and Dynamics of Ice (DESDynI) as tier-1 missions and Lidar Surface Topography (LIST) as a third tier mission. These three missions could all possibly benefit from a very low-noise (near single-photon sensitive), high-bandwidth (1 GHz), near-infrared optical receiver. Improvements in detector quantum efficiency translate directly to reduced laser energy requirements for active laser instruments. This minimizes spacecraft resource requirements (mass, power, volume) and greatly enhances laser and system reliability.

The measurement precision of a laser altimeter is determined by the laser pulse-width and the receiver signal-to-noise ratio (SNR). The SNR is determined by the magnitude of the detected signal photons and noise photons accumulated over the receiver integration time and the additional noise introduced by the detector. Ideally a laser altimeter detector would be able to detect a single photon and attain the near-ultimate receiver sensitivity. The detector should also have a linear output so that the SNR increases with the received signal pulse energy. In addition, it should have a wide dynamic range such that it can achieve the required SNR under the worst-condition measurement environment without introducing adverse effects under the best-condition measurement environment. For a typical Earth-orbiting laser altimeter, the laser return signal dynamic range spans two to three orders of magnitude due to the atmospheric conditions and rapid changing terrain types of the satellite ground track.

All of NASA's space-based laser altimetry missions to date have used versions of the near-infrared enhanced silicon avalanche photodiode (APD) detector manufactured by PerkinElmer Opto-Electronics Canada (a.k.a. EG&G and formerly RCA) for detecting laser signal returns at 1064 nm wavelength. These missions include NEAR, CLEMENTINE, MOLA, ICESAT/GLAS, CALIPSO, MLA and LOLA. The spaceflight optical receivers are based on

custom-built improved versions of the commercial Model C30954E APD. Its RF bandwidth of 140 MHz is matched to the laser transmitter pulse bandwidth. This silicon APD-based optical receiver is described in detail in recent publications[ii,iii].

The laser altimeter system RF signal bandwidth is designed[iv] for a specific spatial resolution and average surface topography roughness. For the space-based ICESat-GLAS instrument, these parameters were 70-meter diameter ground area, surface slope varying from 0-30 degrees and 140 MHz RF signal bandwidth (corresponding to the (-20 dB) bandwidth for a 6 ns laser transmitter pulse width). NASA's future laser altimeters plan to have a higher spatial resolution. A topographic mapping spatial resolution of 5 meters is planned for the LIST mission. This increases the RF (-20 dB) signal bandwidth to greater than 1 GHz and reduces the corresponding laser pulse width to less than 1 ns. The 1 ns pulse width also provides higher height resolution and increased probability of ground location detection under trees for reasonably flat (< 3 degree surface slope) regions.

There are several reasons that make it difficult to extend the near-infrared-enhanced-silicon APD RF bandwidth to 1 GHz. First, a minimum diameter is required to match the laser ground footprint diameter image size for a practical telescope optics f-number. This leads to a larger device capacitance that contributes to the limiting the maximum bandwidth. Second, increasing the device thickness to possibly further enhance the absorption length is not fruitful because it increases the noise current and it increases the electron drift time. Therefore a new detector is required for future NASA lidar missions that require 1 GHz RF bandwidth.

In 2009 we proposed and were awarded a NASA Earth Science Technology Organization (ESTO) Advanced Component Technology (ACT) program to pursue new detector development. Our idea is to use the impact ionization engineered (I^2E) material system in Indium Aluminum Arsenide (InAlAs) to simultaneously achieve high near-infrared quantum efficiency (75%), large diameter (200 μm), > 1 GHz bandwidth and high sensitivity (low-noise – 300 fW/√Hz).

II. INDIUM PHOSPHIDE 140 MHZ BANDWIDTH PHOTO-RECEIVER

Funded by a separate NASA-GSFC program in 2009, Spectrolab built a high-sensitivity modest bandwidth (140 MHz) photo-receiver for use at near-infrared wavelengths. The noise equivalent power (NEP) target for this photo-receiver was 180 fW/√Hz. Spectrolab built this first-generation (Gen1) photo-receiver with an in-hand 200 μm diameter Indium Phosphide (InP) APD and a Philips SA5211 trans-impedance amplifier (TIA). The APD has a lattice matched InGaAsP alloy absorber, which was optimized for 1 um operation.

A. First-generation photo-receiver design and test

The first-generation photo-receiver schematic is shown in Figure 1. The TIA is configured with single-ended AC coupled output to a 50 Ω load. The receiver is assembled into a 14 pin butterfly package with an integrated thermo-electric cooler (TEC) and temperature sensor. A ceramic substrate was designed and fabricated to host the APD, TIA, and all other components. An SMP connector is inserted at the end of the butterfly package to provide the high-bandwidth output. The hermetically sealed package has a lid with an optical window.

A test board was built to enable rapid photo-receiver testing. The test board provides convenient connections to the TEC and temperature sensor, TIA and APD. During the test, an external heat sink was attached to the backside of the butterfly package to extract heat.

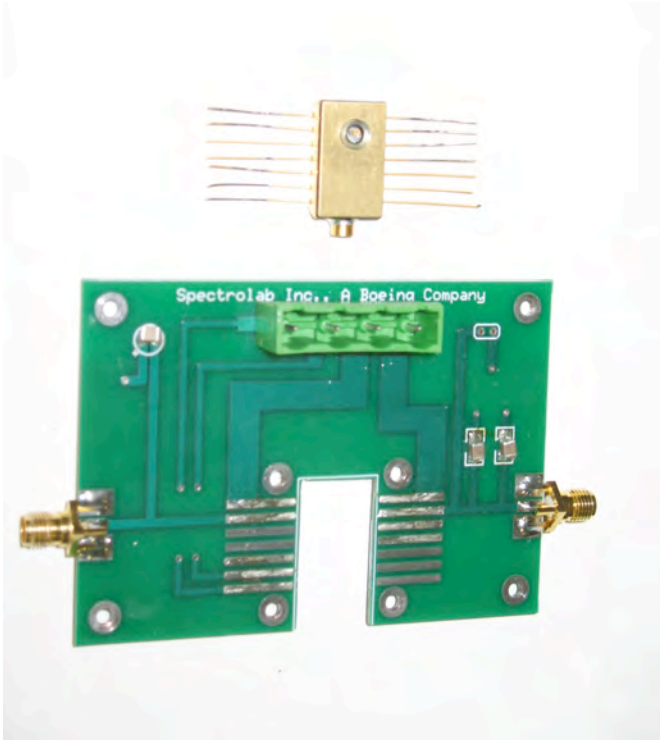

Figure 1. Spectrolab first generation photo-receiver and a test board.

The TIA bias (V_{CC}) range is from 4.5V to 5.5V. The TIA gain is slightly higher with a higher bias voltage. The bandwidth and input-referred current noise are also slightly higher with increasing TIA bias. The APD bias voltage is applied through a low-noise power supply with current compliance in order to ensure proper receiver operation. During our test, 20μA compliance was used.

The photo-receiver bandwidth is limited by the Philips TIA bandwidth (not the InP APD bandwidth). However, operating the receiver at lower temperature increases the

response bandwidth to higher than 180 MHz realized at room temperature. The TIA trans-impedance is measured about 7.8 kΩ in the single-ended output configuration. Thus the photo-receiver responsivity is $R_{sp,APD} \times M \times 7.8\ k\Omega$. With an APD gain equal to 30, the photo-receiver responsivity is about 130 kV/W.

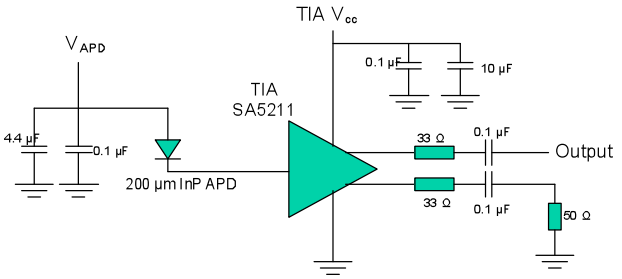

Figure 2. Schematic of Spectrolab first generation photo-receiver.

The receiver noise is characterized with a high-bandwidth oscilloscope with histogram function. The photo-receiver output is connected to an oscilloscope. The input voltage histogram had a Gaussian distribution with a standard deviation σ_V that is dominated by the noise voltage of the photo-receiver. The photo-receiver noise voltage was measured in the dark as a function of APD gain. The NEP is calculated by $\sigma_V/(R_{sp,receiver} \times \sqrt{\text{bandwidth}})$. The result is shown in Figure 4. The lowest NEP is about 300 fW/√Hz.

Engineers from NASA-GSFC illuminated the same photo-receiver with 100 ns light pulse with a repetition rate of 1MHz. Histograms are measured at both light on and light off condition. The signal-to-noise ratio (SNR) was calculated from the mean output voltage pulse height and the noise of the output signal. The NEP is calculated from the normalized laser pulse power/SNR/√Bandwidth. The minimum NEP measured at NASA-GSFC is 230 fW/√Hz. The lower NEP could be the result from a bandpass filter in NASA's test setup.

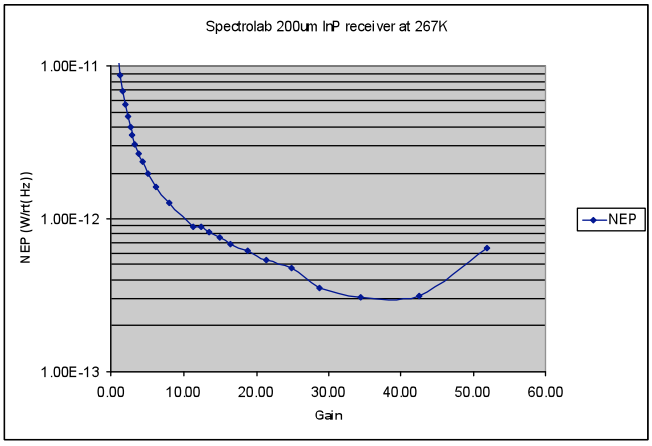

Figure 4. Spectrolab 200µm InP photo-receiver versus APD gain.

B. Photo-receiver improvement

The noise equivalent power (NEP) of a photo-receiver is given by:

$$NEP = \frac{h\nu}{\eta_{QE}} \left[2qI_d F + \frac{\alpha^2}{M^2} \right]^{1/2} \qquad (1)$$

where F is the APD excess noise factor given by:

$$F = kM + (2 - \frac{1}{M})(1 - k) \qquad (2)$$

where h is the Boltzmann constant, ν is the optical frequency, η_{QE} is the APD quantum efficiency, q is electron charge, I_d is the APD dark current, M is the APD internal multiplication gain, α is the TIA's input noise current, k_{eff} is the ratio of electron and hole ionization coefficients.

From Eq. (1), the most straight-forward path to reduce the NEP is to increase the APD quantum efficiency, η_{QE}. The InP APD has a quantum efficiency about 64% at 1.06 µm. By using an APD with quantum efficiency of 75%, the NEP will be reduced by 17%. The APD in the prototype receiver was front side illuminated. An alternative configuration is to introduce the light from backside of the substrate and put a mirror on top of the mesa to introduce a reflection. Backside illumination then would effectively double the absorption path and will increase the detector's quantum efficiency. The thickness of the absorber can also be increased to achieve even higher quantum efficiency.

At an APD gain (M) less than 40, the photo-receiver noise is dominated by the TIA noise. For a given bandwidth, the TIA with lowest current noise should be used. Operating the TIA at a lower temperature, (e.g. 240 K), will reduce the input referred noise by about 10% from its room temperature value.

From Eq. (1), reducing the APD excess noise (F) will significantly reduce the NEP (i.e. improve the photo-receiver sensitivity). From Eq. (2), F is reduced by reducing the k_{eff}. The ionization coefficient, k_{eff}, is a material parameter that can be reduced through material engineering. In the next section, we described further reduction of k_{eff} (and ultimately the NEP) through custom material engineering.

III. LOW EXCESS NOISE APD WITH IMPACT IONIZATION ENGINEERING

APDs are widely used to improve the photo-receiver SNR because of their internal high gain. However, the avalanche process introduces excess noise that is a function of gain

and ultimately limits photo-receiver sensitivity. Ideally, only one carrier, either electron or hole, would trigger the impact ionization to minimize excess noise. Silicon has very low k_{eff} (0.02) and is widely used in low-noise photo-receivers operating in the visible spectrum. The most common multiplier semiconductor compound for the near-infrared (< 1.7 μm) sensitive III-V APDs are InP with a k_{eff} equal to 0.45 and InAlAs with k_{eff} equal to 0.22. APDs with thin multipliers show smaller k_{eff} value than the corresponding bulk material[v]. However, there are practical limitations on fabricating very thin multiplier avalanche photodiodes that result in higher tunneling currents and increased noise as well as steep voltage-gain characteristics that require bias voltage stabilization. Another approach is impact ionization engineering (I^2E). I^2E is an approach to combine materials with different impact ionization threshold energies in the multiplication region. It is worth to note that the impact ionization threshold energies are not the same as the material's bandgaps. With proper design, the impact ionization events can be localized in the material with lower threshold energy. There, these impact ionization events show some increased degree of determinism, which is equivalent to a lower effective k value than would be otherwise realized. Such APDs have been demonstrated and a k_{eff} about 0.1 was realized[vi].

A. Intrinsic InAlAs APDs

Spectrolab has been developing InAlAs since 2003. Very low dark current discrete APD and APD arrays have been developed for various applications. The effective k value is about 0.22 for InAlAs APDs.

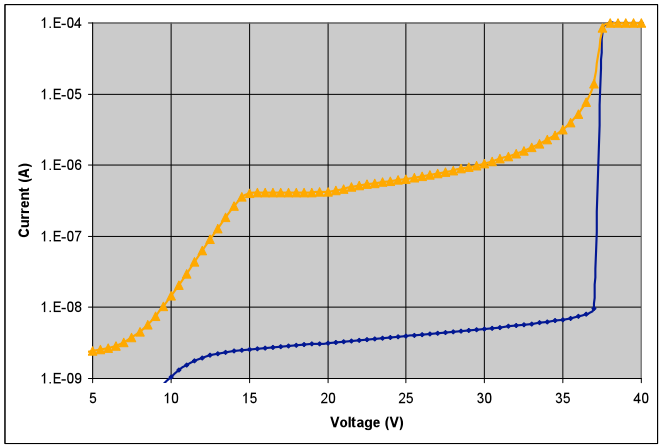

Figure 5. Typical Spectrolab 75μm InAlAs APD current voltage characteristics.

In this investigation Spectrolab baseline InAlAs APDs were grown on InP substrates. The baseline APD has a p on n configuration and the charge layer is doped with zinc to control the electric field profile. The absorber is lattice matched InGaAs. Details on the growth and fabrication of these APDs are discussed in Ref. 8.

B. I^2E InAlAs APDs

On the ESTO ACT program we are optimizing I^2E APDs for operation at 1 μm wavelength. The multiplier is a combination of InAlAs and InGaAlAs. The InGaAlAs alloy has smaller impact ionization threshold energy than InAlAs. To simplify the material growth, the absorber is comprised of an InGaAlAs alloy with a bandgap of 1.05 eV. For the multiplier, the InGaAlAs alloy was tuned to have a bandgap about 1.2 eV. Both alloys are lattice matched with InP substrate. The APDs are grown in production MOVPE reactors at Spectrolab.

I^2E APD structures are shown in Figure 6. A thin InGaAlAs layer was inserted into the InAlAs multiplier to implement the I^2E design. Wafers from two separated growth run have been fabricated. The APD dark currents are at most a few nA before breakdown. For an APD with 75μm diameter, the multiplied dark current at gain of 1 is about 80 pA for device A and 300 pA for device B at room temperature.

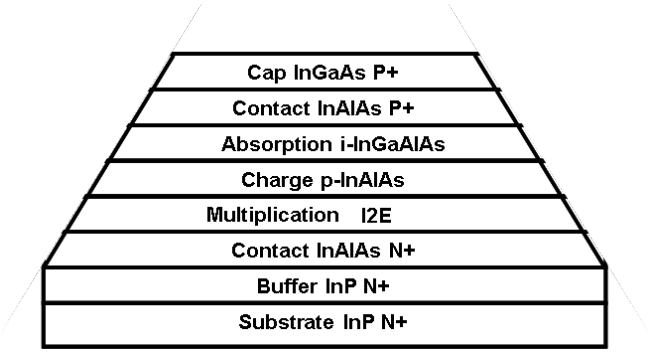

Figure 6. I^2E APD structures.

The excess noise factors of the I^2E APDs were measured at University of Virginia with an HP8970B noise figure meter. An Argon ion laser with wavelength 351/363nm was used to illuminate the APDs. The UV laser ensures pure electron injection into the multiplier. Measurement details have been discussed in a previous publication[vii].

Figure 7 displays the measured excess noise versus gain characteristics collected on two I^2E APDs. This figure also displays excess noise factors as calculated from Equation 2 for several different effective k values. Both I^2E APDs show effective k-values less than 0.1 for optical gains up to 7. The measured excess noise is much lower than previously measured[viii,9] InAlAs APDs with k_{eff} values of about 0.22. Combined with very low dark current, these APDs are good candidates for high sensitivity photo-receivers. In reality, the TIA current noise is the dominant noise source when the APD gain is low. Thus the APD should be biased at a gain as high as possible until the APD excess noise suppresses the TIA noise. Based on the trend, at higher gain, the APDs still show an effective k value less than 0.15. Continuing studies are way to optimize the I^2E structure to increase the gain and reduce k value further. The first growth of this APD design suffers from early breakdown in the lower

bandgap InGaAlAs layer resulting in limiting the gain to less than 7. Our second growth will eliminate this issue. We are also focused on further optimization of the quaternary layer.

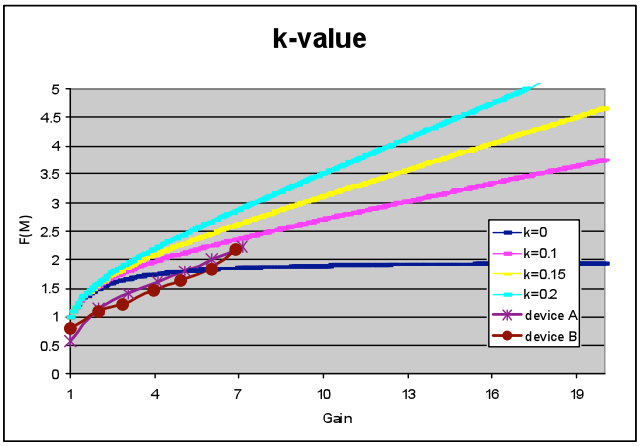

Figure 7. Excess noise factor of two I2E APDs.

Spectrolab is currently working on 2nd generation photo-receiver, which has the I^2E low excess noise APD and 1 GHz bandwidth TIA. In Figure 8, the NEPs are calculated based on various k-value and TIA input-referred noise currents. An APD responsivity of 0.7 A/W was used in the calculation. The goal is to develop a photo-receiver with NEP of ≤ 300fW/√Hz over 1 GHz bandwidth.

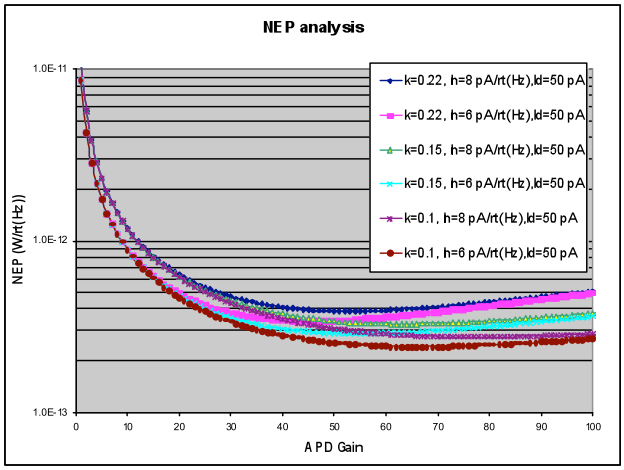

Figure 8. NEP analysis for a photo-receiver with I^2E APD and GHz TIA.

ACKNOWLEDGMENT

We greatly appreciate the support of the NASA ESTO ACT program that is funding this work. The authors would like to thank Prof. Campbell's group at University of Virginia for the excess noise measurements.

REFERENCES

[i] *Earth Science and Applications from Space: National Imperatives for the Next Decade and Beyond*, National Research Council of the National academies, The National Academies Pres, Washington D.C., (2007).

[ii] M.A. Krainak, X. Sun, G. Yang, L.R. Miko, and J.B. Abshire, "Photon detectors with large dynamic range and at near-infrared wavelength for direct detection space lidars" Proc. SPIE 7320, 732005 (2009)

[iii] M.A. Krainak, X. Sun, G. Yang, and W. Lu, "Comparison of linear-mode avalanche photodiode lidar receivers for use at one-micron wavelength" Proc. SPIE 7681, 76810Y (2010)

[iv] C.S. Gardner, "Target signatures for laser altimeters: an analysis" Applied Optics Vol. 21, No. 3 pp. 448-453 February 1982.

[v] J. Campbell, S. Demiguel, F. Ma, A. Beck, X. Guo, S. Wang, X. Zheng, X. Li, J. Beck, M. Kinch, A. Huntington, L. Coldren, J. Decobert, and N. Tscherptner, "Recent advances in avalanche photodiodes", J. Sel. Topics Quantum Electron. Vol. 10, No. 4, 777 (2005)

[vi] N. Duan, S. Wang, F. Ma, N. Li, J. C. Campbell, C. Wang, and Larry A. Coldren "High-Speed and Low-Noise SACM Avalanche Photodiodes With an Impact-Ionization-Engineered Multiplication Region" IEEE Phot. Tech. Lett 17, 1719 (2005).

[vii] Xiangyi Guo, Ph. D. dissertation, "High Performance Ultraviolet 4H-SiC Avalanche Photodiodes", 2005

[viii] J. Boisvert, G. Kinsey, D. McAlister, T. Isshiki, R. Sudharsanan and M. Krainak; "Large Area InAlAs/InGaAs Single Photon Counting Avalanche Photodiodes" Proc. SPIE Laser Radar Technology and Applications IX p. 126 (2004).

[9] J.C. Dries, K. J. Thomson and S.R. Forrest; "In0.53Ga0.47As/In0.52Al0.48As separate absorption, charge, and multiplication layer long wavelength avalanche photodiode" Electronics Letters, Vol.35, No. 4, p. 334 (1999).